Research Article

Investigating Induced Thermal Shock Stresses on Washing Machine Glass with Finite Element Analysis

Ozan Kovancı[1*], Muharrem Erdem Boğoçlu[2*]

[1] Yıldız Technical University, Orcid ID: https://orcid.org/0000-0002-6388-8794, ozan.kovanci@std.yildiz.edu.tr
[2] Yıldız Technical University, Orcid ID: https://orcid.org/0000-0002-5021-5865, bogoclu@yildiz.edu.tr
[*] Correspondence: ozan.kovanci@std.yildiz.edu.tr

(First received January 16, 2023 and in final form March 18, 2023)

Reference: Investigating Induced Thermal Shock Stresses on Washing Machine Glass with Finite Element Analysis. The European Journal of Research and Development,3(1), 16–30.

Abstract

Glass has become an increasingly popular material in modern home appliances due to its sleek, aesthetic appearance and durability. Washing machine manufacturers have followed this trend, incorporating glass as a key component in their designs. However, glass door breakage failure is a common issue that can cause serious injuries and damage. Glass door failure can occur suddenly or gradually and can be caused by several factors, including thermal shock, impact, wear and tear, and manufacturing defects. Understanding the failure modes of washing machine glass doors is crucial for developing effective solutions to prevent glass door failure in washing machines. The most common failure of glass in washing machines is subjected to repeated thermal shocks due to the frequent fluctuations in temperature during the washing and drying cycles. This thermal stress can cause the glass to crack, leading to safety hazards and costly repairs for consumers.

The aim of this paper is to investigate the induced thermal shock stresses on washing machine glass and to propose potential solutions to mitigate the risk of glass breakage. The study will be carried out through a combination of experimental data collecting and numerical simulations including washing cycle simulation and experimental test scenario. The numerical simulations will use finite element analysis to model the thermal stresses experienced by the glass during the washing and drying cycles.

This paper is organized as follows. At the first part, the study will provide a literature review of existing research on thermal shock in glass and its effects on washing machines. Secondly, it will present the methodology used in this study, including details on the numerical simulations and experimental testing. Third part, covers the presentation of the results of the study, including the stress profiles of the glass samples and the observed damage. Fourth part will discuss the implications of the results and propose potential solutions to mitigate the risk of glass breakage in washing machines. Final part will conclude the paper with a summary of the key findings and suggestions for future research.

Overall, this study seeks to contribute to the development of safer and more reliable washing machines, by shedding light on the thermal shock stresses experienced by the glass components and proposing solutions to mitigate the associated risks.

Keywords: *Thermo-mechanical analysis, finite element analysis, thermal shock, glass*

1. Introduction

Glass is a widely used material in the manufacturing of household appliances due to its transparency, durability, and aesthetic appeal [1]. Washing machines are no exception, as they often feature glass windows that allow users to view the washing process. However, glass can be susceptible to thermal shock, a phenomenon that occurs when the temperature of a material changes rapidly, causing uneven expansion or contraction.

In washing machines, thermal shock can occur when the hot water used for washing comes into contact with the cool glass window. This sudden change in temperature can result in thermal stresses that can weaken the glass, leading to cracking or even shattering. The failure of the glass window not only leads to safety concerns but also affects the aesthetic and functional aspects of the washing machine.

To ensure the safe and reliable operation of washing machines with glass windows, it is essential to investigate the thermal stresses induced in the glass due to thermal shock. In this paper, we aim to investigate the thermal shock stresses on washing machine glass through experimental and numerical analyses. We will analyse the impact of various parameters such as water temperature, glass thickness, and cooling rate on the induced stresses. Additionally, we will investigate the effects of different glass compositions and properties on thermal shock resistance.

This study also consist of literature review is to investigate the induced thermal shock stresses on washing machine glass. To discuss the current knowledge on thermal shock resistance of glass and the existing studies related to this topic.

In the study by Guo et al. (2010) titled "Thermal stress analysis of a glass plate with a hole under different cooling conditions," the authors conducted a numerical simulation to investigate the thermal stress distribution in a glass plate with a hole. The study revealed that the stress distribution in the glass plate was affected by the cooling rate and the hole size [1]. Hamidouche et al. (2013) conducted a study titled "Thermal shock resistance of a soda-lime glass." In this study, the thermal shock resistance of soda-lime glass was investigated using a water quench test. The results of the study showed that the thermal shock resistance of the glass was influenced by the cooling rate and the microstructure of the glass [2]. In the study by Wondimu et al. (2003) titled "Thermal shock resistance of porous ceramics," the authors investigated the thermal shock resistance of porous ceramics. The study used numerical simulations to determine the thermal shock resistance of the ceramics. The results showed that the thermal shock resistance of the ceramics was influenced by the porosity and the cooling rate [3]. In the study by Wang et al. (2018) titled "Thermal shock resistance of multi-bonded SiC ceramics," the authors investigated the thermal shock resistance of multi-bonded SiC ceramics. The study used numerical simulations to determine the thermal shock resistance of the ceramics. The results showed that the thermal shock resistance of the ceramics was influenced by the microstructure and the cooling rate [4]. In the study by Rokosz et al. (2017) titled "Thermal Shock Resistance of Ceramic Materials: A Review," the authors reviewed the literature on the thermal shock resistance of ceramic materials. The study highlighted the importance of understanding the thermal shock resistance of ceramics in various applications, including high-temperature applications and space exploration [5].

Although the literature review reveals several studies on thermal shock resistance of glass, there is a gap in the literature concerning the thermal shock resistance of washing machine glass. Washing machine glass is subjected to various hazardous cycle scenarios, which can induce thermal shock stresses on the glass. To the best of our knowledge, there is no study in the literature that investigates the thermal shock resistance of washing machine glass under the most hazardous cycle scenarios.

Therefore, the proposed study is significant as it aims to investigate the induced thermal shock stresses on washing machine glass by conducting FEM on complex geometry glass subjected to the most hazardous cycle scenarios of washing machines. Additionally, the proposed study will develop an experimental test scenario that will be compared to the real-time washing scenario, providing a more accurate evaluation of the thermal shock resistance of washing machine glass.

The findings of this study will provide valuable insights into the behavior of washing machine glass under thermal shock conditions and help manufacturers optimize their designs to enhance the safety and durability of their products. Moreover, the results of this research can be extended to other applications that involve glass and thermal shock, such as automotive and architectural glass.

2. Materials and Methods

The aim of this study is to determine the thermally induced stress on the washing machine’s glass door by the means of Finite Element Analysis (FEA). In order to achieve this precisely, real-time temperature vs time data should be collecting with an experimental set-up. After collecting the required data for the most hazardous working conditions, FEM model was built and simulations obtained by simplified models and assumptions to be on focus on the study.

2.1. Experimental Data Collection

The standard washing machine programs may vary depending on the manufacturer and model of the washing machine, but generally, most washing machines have the following basic programs such as cotton 60, cotton 90, eco, synthetics, delicates, hand wash, quick wash, heavy duty and rinse & spin. To identify the worst case in a practical way; thermal camera observation was carried out by *Fluke Thermal Imager* equipment for all type of washing program. *Figure 1* shows the visualisation of cotton 60° program. First visual shows the starting point of the thermal imaging which is around 20-22° C. Afterwards, the washing cycles run one by one to detect the highest temperatures, for instance cotton 60 program, washing machine glass were reached to 60° C, immediately after the cold water poured inside and the temperature dramatically down around 40° C, then gradually cooled around 25° C.

However, there are some positive and negative aspects of thermal imaging. Firstly, there were no numerical data for calculating the induced thermal stress among the washing cycle. Secondly, thermal imaging was not able to show the temperature differences of internal and external surfaces separately. Despite all these facts, there could be more than 30 different washing programs in washing machines and with the help of thermal imaging; the riskiest washing cycle was appointed readily and effectively in a short span of time. As a result of this observation; the riskiest program found out as of Cotton 90. All of the FEM analysis carried out in Cotton 90 washing program because of the dramatic cooling rate compared to all other washing programs.

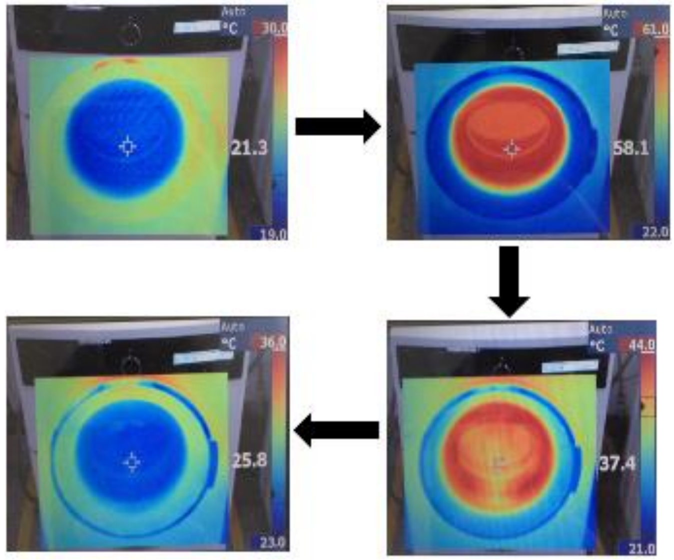

Figure 1: Thermal Imaging of Cotton 60 washing cycles (By permission of Vestel Co.)

To investigate the induced internal and external surface of the washing machine glass door in detail, a new experimental procedure was designed. 20 thermocouples were positioned on the glass door that simulates the system ideally. 12 pieces were positioned internal surface (water side) and the remaining 8 pieces were fixed on the external surface (air side) of the glass door.

Figure 2: Thermal Imaging of Cotton 60 washing cycles (By permission of Vestel Co.)

Figure 2 represents the experimental set-up and the positions of the thermocouples where were located both inside and outside surface of the washing machine glass door. *Hioki data logger* was used to collect the required temperature measurements during each washing cycles.

The temperature curves of all thermocouples might be seen on the *Figure 3*. The obtained curves were fitted with a *Matlab R 2019* algorithm to be used in the finite element analysis.

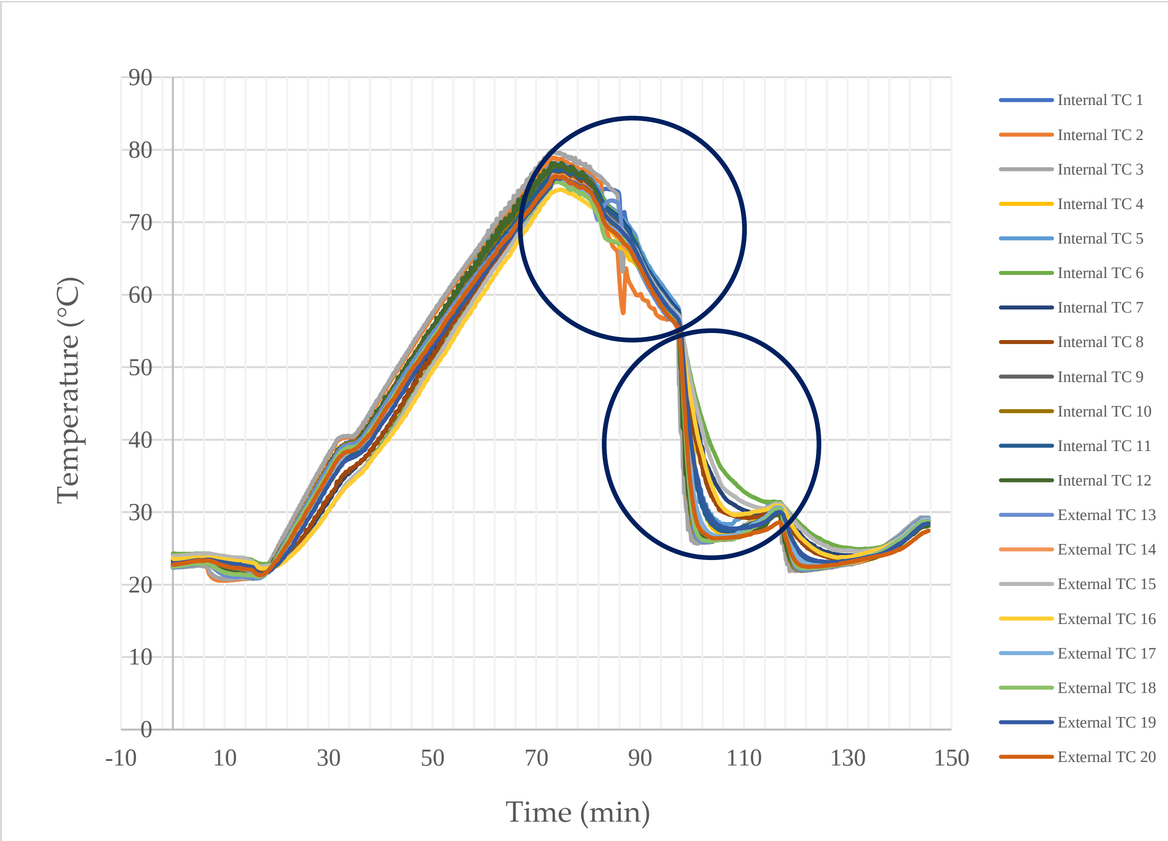

Figure 3: Temperature vs time measurements results for Cotton 90. (By permission of Vestel Co.)

2.2. Finite Element Analysis

The thermal stress analysis was carried out in order to assess the effect of temperature gradients across the surface and within the thickness of the glass door which arise during the washing cycles or while testing. Thus, for the calculation of the ensuing stress in the glass door, it is considered both the thermal data (temperatures vs. time) that was measured on the glass' air-side and water-surfaces during the washing cycles and the temperature induced during the thermal shock test (rapid cooling of the waterside surface). The geometry of the glass door adopted for the finite element analysis was based on the 3 dimensional CAD data in visualized *Figure 4*.

The glass thickness distribution used in the models was assumed to be equal to the nominal one found in the drawing, i.e. 5.3 mm for the flange and 5 mm for the remaining parts, corresponding to a glass weight of 1.45 kg. It should be noted that the current analysis doesn't take into account severe damage, either created during glass manufacturing or resulting from abusive handling, since it was assumed the glass object will be manufactured and handled properly. Moreover, the effect on any decorative elements (either moulded into the item as embossing or added subsequently as enamelling) are not considered in the following analysis.

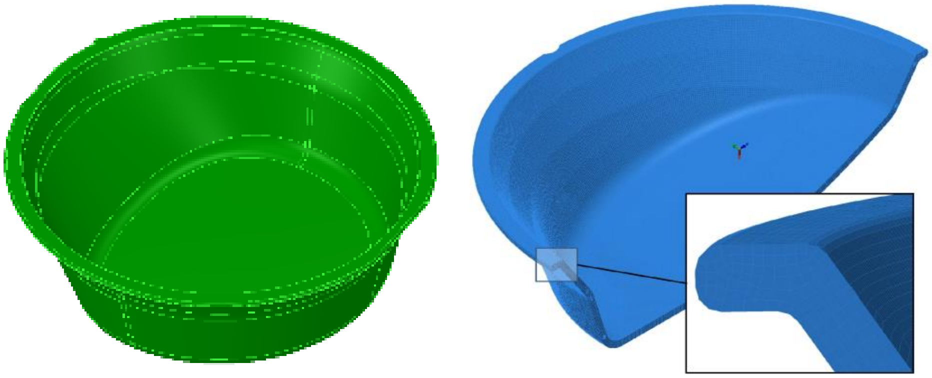

Figure 4: 3D CAD model of the glass door (By permission of Vestel Co.)

The 3D model, made by 383.550 brick-dominating elements, was meshed paying great attention to have an appropriate number of elements' layers (6 in this case) through the thickness. Indeed, during thermal shock a steep gradient of temperature and stresses arise within the thickness, thus, having an adequate mesh, is fundamental for obtaining reliable results. Two different load cases were taken into account:

a. **LC1 - Washing cycle simulation**: the measured data was analysed and used to define the surface temperatures to be applied to the model. This allows us determining the glass door behaviour with an asymmetric thermal service load;
b. **LC2 - Experimental test scenario:** the glass door is quenched from the uniform temperature of 80°C by soaking it in a colder water bath at the constant temperature of 20°C.

This allows to determine the glass door's stress field generated during thermal-shock testing according to a given procedure and compare it with the stress field previously obtained. Due to the asymmetric temperature field measures during the washing cycles, two different finite element models were made. For each load case, two simulations were studied: a transient heat transfer simulation for determining the temperature distribution on the whole volume of the glass door; another non-linear mechanical event simulation for analysing the ensuing stress field. The following thermal and static finite element analyses were carried out with the *Autodesk Simulation Mechanical* software. The evaluation of the stresses due to the reference thermal loads, was performed using the characteristic properties of silica-soda-lime glass reported in *Table 1*.

Due to the complexity of reproducing, in a reliable way, the washing scenario to obtain the temperature distribution on the glass door, starting from the local values obtained by the thermocouples, it is considered that the following assumptions and simplifications of the real phenomenon. The measured Cotton 90 cycle’s temperatures show that the temperature distribution is asymmetric. In these parts of the model, two different convection loads were applied. Depending on the considered glass door side (water- or air-side), two different heat convection coefficients (temperature independent), and ambient temperature (variable with time, obtained from the lower temperatures measured in proximity) were used.

Table 1: Characteristic Properties of Soda Lime Glass

Variables	Sign	Unit	Value
Density	ϱ	kg/m^3	2500
Young's Modulus	E	MPa	7000
Poisson's Ratio	μ	-	0,23
Specific Heat Capacity	c	J/(kg K°)	862
Thermal Conductivity	λ	W/(m K°)	0,91
Thermal Expansion Coefficient	α	$°C^{-1}$	$8,87.\ 10^{-6}$

3. Results

Transient heat transfer analysis was performed with assumptions in order to obtain the temperature distribution on the whole solid domain. The finite element analysis began after the first heating phase, thus we assumed an initial temperature of 64°C for the whole door. Then, during the hot phase, the surface temperatures were applied to the glass door to obtain the non-uniform (through the volume) thermal equilibrium before its cooling.

The surface temperatures at three different time intervals (t_0, t_1 and t_2); instant t_0 corresponds to the end of the hot phase (~ 82 min actual time), before the cooling induced by the first inlet of water; t_1 and t_2 correspond to ~ 92 and 95 min (actual time) after the start of the washing cycle, i.e., immediately after and during the second cold water inlet, instants in which the tensile stresses reach the maximum values.

The same FE model was used to perform a thermal stress analyses starting from the results of the unsteady heat transfer analysis: the nodal temperatures were used in a mechanical non-linear model *Mechanical Event Simulation*, to determine the correlated stress field. The model is constrained by: rollers on one edge of the sidewall/flange connection in order to prevent the translation in the direction orthogonal to the flange plane; one hinge at one node to prevent rigid body motion in the flange plane.

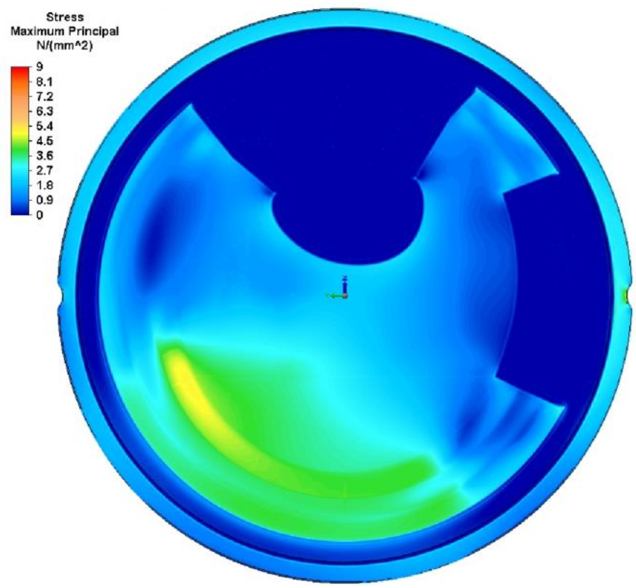

Figure 5: Maximum principal stress distribution on the air-side at t_2.

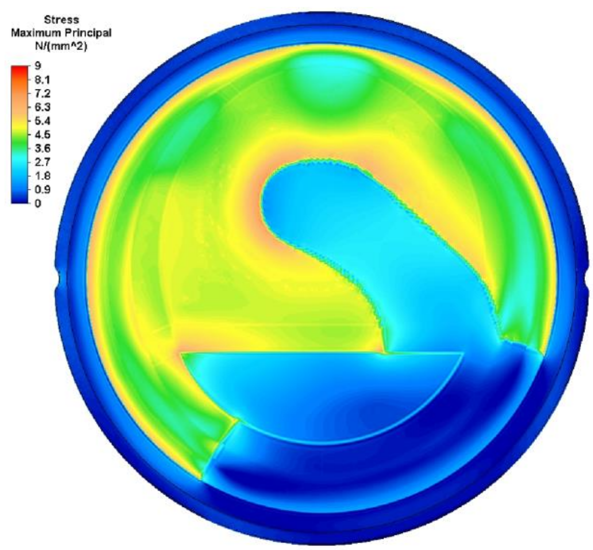

Figure 6: Maximum principal stress distribution on the water-side at t_2

The highest values of the maximum principal stress are achieved when, on each surface, the maximum temperature difference is reached (~ 10° C). *Figure 5* and *Figure 6* show how the stress field changed respectively on the air-side and water-side, respectively. In both cases the maximum stresses arise in the colder zones, i.e., the lower area on the air-side and the higher area on the water-side ($\sigma_{11} < 8$ MPa, $\sigma_{22} < 5$ MPa). The maximum principal stress on the flange is less than 1 MPa before t_2, then suddenly the maximum stress reaches ~ 7 MPa at the lateral surface of the positioning grooves.

The FE models showed that, with the assumed thermal history at the pertinent zones, the stress field resulted to be, almost always, not equi-biaxial and lower than 10 MPa. More in detail, the maximum stress on the air-side is achieved in hot phase and persists for almost its duration. The highest stresses on the water-side surface and flange were found after the second cold water inlet at t_2, when the maximum temperature difference between zones is reached. These stresses last some minutes only. Both for the air- and water-surface, the tensile stresses arise in the colder areas.

During the washing cycles, the presence of tensile stresses on the glass door is not connected to the rapid cooling of one surface, as happens in cold thermal shock, but they are induced by the temperature's dissimilarities between different zones: warmer parts try to expand while the cooler ones try to shrink. The mutual strains cause the rise of the stresses.

The 3D Finite Element model previously employed for the transient heat transfer analysis was also used in a mechanical non-linear model by *Mechanical Event Simulation* for analysing the stress field induced by the numerically evaluated temperatures. The model is constrained by: rollers on one edge of the sidewall/flange connection in order to prevent the translation in the direction orthogonal to the flange plane; one hinge at one node to prevent rigid body motion in the flange plane; a symmetry constrain on the nodes contained in the symmetry plane. The stress field caused by the temperature distribution, obtained by the FE analysis are summarized in the next figures.

Figure 7 and *Figure 8* show the distribution of the maximum principle stress after 2.7 s from the beginning of the cooling, when the maximum values of tensile stress were achieved. The maximum stresses on the outer surface were found at the sidewall (~25 MPa) even if similar tensile stresses were obtained also in the other areas of the water-side surface. The stress field resulted to be equi-biaxial in almost all the zones of the water-side surface except the sidewall and the sidewall/flange connection of the glass door.

The stress field in the centre of the glass door and at the centre/sidewall connection is uniform (respectively $\Delta\sigma_{11}$, $\Delta\sigma_{22} < 2.7$ MPa; $\Delta\sigma_{11} < 3$ MPa and $\Delta\sigma_{22} < 4.5$ MPa). Lower uniformity of the stress field was found in the remaining zones, for both the maximum and the intermediate principal stresses: sidewall, $\Delta\sigma_{11} < 5.7$ MPa; $\Delta\sigma_{22} < 14.7$ MPa; sidewall/flange, $\Delta\sigma_{11} < 12.2$ MPa; $\Delta\sigma_{22} < 9.9$ MPa. Differently from what was found in the LC1-washing cycle simulation, the air-side surface is almost always in compression or stress free: moderate tensile stresses ($\sigma_{11} < 6$ MPa, t = 2.7 s) can be observed at the lower sidewall, near the sidewall/flange connection.

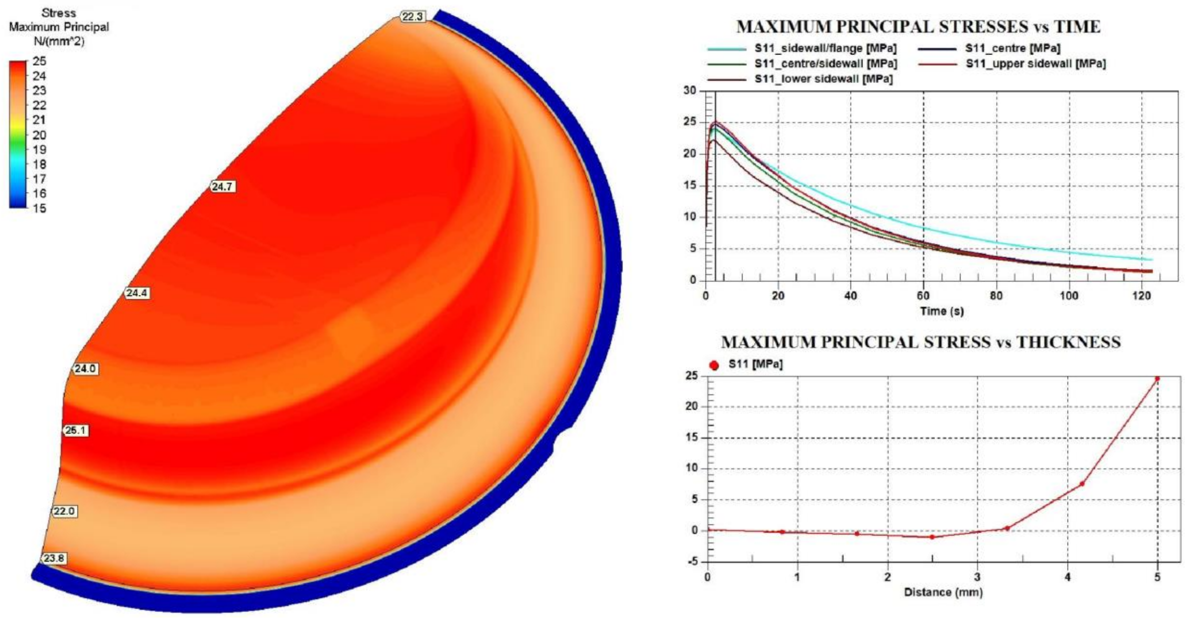

Figure 7: Maximum principal stress distribution on the water-side surface (t = 2.7 s)

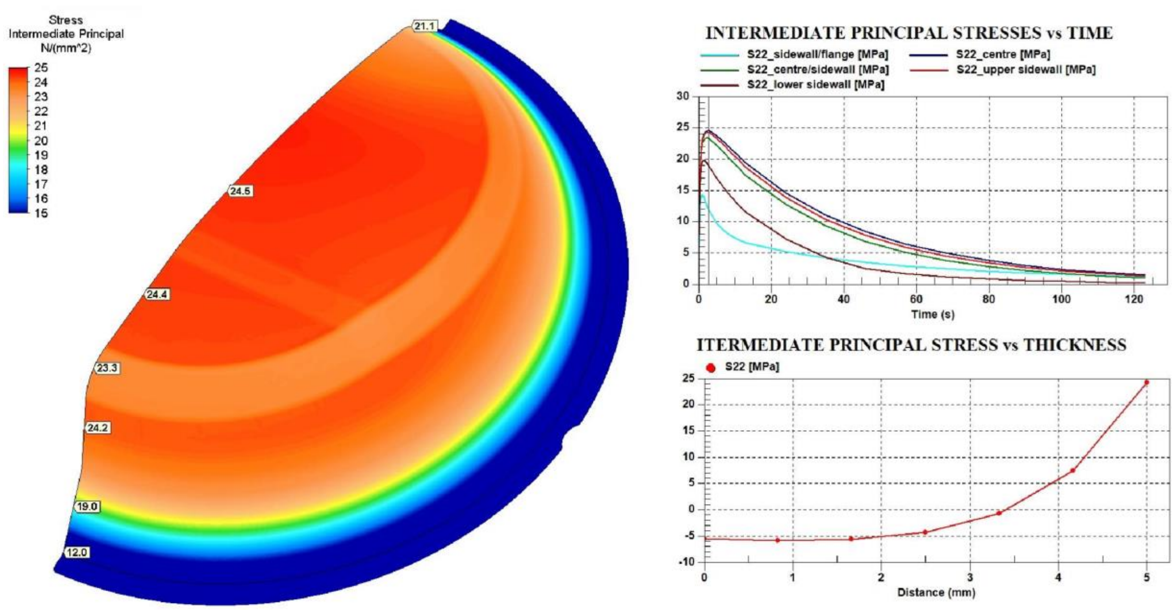

Figure 8: Intermediate principal stress distribution on the water-side surface (t = 2.7 s).

Similar FE analysis have been performed to evaluate the stress field generated in the different glass door zones when higher ΔT are applied, during the thermal shock test, to the water-side surface. The results are reported in *Table 2*.

Table 2: Maximum principal stresses evaluated for different applied thermal shock temperatures

Zones	ΔT = 60 °C @ 2.7 s		ΔT = 90 °C @ 2.1 s	
	σ_{11} [MPa]	σ_{22} [MPa]	σ_{11} [MPa]	σ_{22} [MPa]
Center	24,9	24,6	39,3	38,9
Centre/Sidewall	24,6	24	38,8	38
Sidewall	25,1	24,3	39,6	38,3
Sidewall/Flange	24,9	16,3	39,2	26,7

4. Discussion and Conclusion

The results and discussion of the academic paper present the findings of Finite Element (FE) simulations of washing cycles (LC1) and thermal shock (LC2) on glass doors. The study reveals that the measured temperature variation induces moderate tensile stresses on the glass door, which are always lower than 10 MPa, even though the temperature difference between hot glass and cold water is around 60°C. The maximum stress on the air-side is observed during the hot phase and persists for almost its duration. The highest stresses on the water-side surface and flange occur after the second cold water inlet when the maximum temperature difference between zones on the same surface is reached. The tensile stresses arise in the colder areas both on the air and water-surface. The presence of tensile stresses on the glass door during washing cycles is not related to the rapid cooling of one surface as in cold thermal shock, but is induced by the temperature gradient between different zones. Lowering the stresses could be achieved by reducing the temperature differences within each surface.

The study also shows that the stress field generated during a thermal shock is characterized by an almost uniform and bi-axial tensile stress on the quenched surface, which is the ideal condition for testing glass strength. The condition allows us to have results less sensitive to crack orientation, except on the sidewall/flange zone. Performing a thermal shock with a nominal temperature difference of 60°C observed during washing cycles causes maximum principal stress of around 25 MPa at the sidewall, which is about three times higher than the stress level estimated in LC1 analysis. Similar tensile stresses are obtained in other areas of the water-side surface. The higher thermal stresses are caused by the steep thermal gradient generated within a tiny layer at the water-side surface. The expected stress is influenced by the applied temperature difference, glass thermal conductivity, surface convection coefficient, and glass thickness. The thermal shock test condition is more severe than the real washing cycle.

The study suggests that the maximum stresses found in the LC1 analysis are not enough to cause glass breakages unless heavy defects are present during glass production, handling, mounting, or in-service damages. The critical flaw size is calculated using fracture mechanics equations, indicating that breakage occurs at 10 MPa only if a very deep critical flaw exists. All cracks with a depth smaller than 0.2 mm will not propagate due to static fatigue phenomenon.

Furthermore, according to the NASA Technical Standard STD-5018, the optimal level of residual compressive stress should be two times the applied limit surface tensile stress. For LC1, a minimum residual compression value of 20 MPa should be induced on the glass during tempering [7]. This value is lower than what is reported for flat glass in the ASTM Standard C 1048-12 [8]. Therefore, the tempering level should be chosen considering the glass producer's experience and knowledge of its tempering process, looking for the higher compressive residual stresses with no surface tensile stress outcropping. Considerations regarding the expected fragmentation level at breakage should also be taken into account. From the thermal load/stress point of view, the LC1 analysis suggests that a heat-strengthened glass could be enough if no excessive defects/damages are present on the surfaces.

5. Acknowledge

The authors would like to thank Vestel Washing Machine R&D Center's executives and engineers for their valuable support during the data collecting phase of the study.

References

[1] Khare, S. [1] Le Bourhis, E. (2014). Glass Mechanics and Technology (2nd Edition). Wiley-VCH. https://doi.org/10.1002/9783527679461.

[2] Dubé, M., Doquet, V., Constantinescu, A., George, D., Rémond, Y., & Ahzi, S. (2010). Modeling of thermal shock-induced damage in a borosilicate glass. Mechanics of Materials, 42, 1017-1026. https://doi.org/10.1016/j.mechmat.2010.07.002

[3] Hamidouche, Z., Mohamed, H., Bouaouadja, N., Chevalier, J., & Fantozzi, G. (2013). Thermal shock resistance of a soda lime glass. Ceramics Silikaty, 57, 39-44. https://doi.org/10.1007/s10853-018-2229-1

[4] Mackerle, J. (2002). Finite element analysis and simulation of quenching and other heat treatment processes: A bibliography (1976–2001). Computational Materials Science, 24(2), 141-165. https://doi.org/10.1016/S0927-0256(01)00219-5

[5] Kozłowski, M., Bedon, C., & Honfi, D. (2018). Numerical Analysis and 1D/2D Sensitivity Study for Monolithic and Laminated Structural Glass Elements under Thermal Exposure. Materials, 11(9), 1531. https://doi.org/10.3390/ma11091531

[6] Karlsson, S. (2017). Spontaneous Fracture in Thermally Strengthened Glass - A Review and Outlook. Ceramics-silikaty, 61(3), 188-201. https://doi.org/10.1016/j.jeurceramsoc.2014.07.001

[7] National Aeronautics and Space Administration. (2013). NASA Technical Standard STD-5018, Strength Design and Verification Criteria for Glass, Ceramics, and Windows in Human Space Flight Applications. https://standards.nasa.gov/standard/std5018

[8] ASTM International. (2012). ASTM Standard C 1048-12, Standard Specification for Heat-Strengthened and Fully Tempered Flat Glass.